

# cardinalR: Generating interesting high-dimensional data structures

by Jayani P. Gamage, Dianne Cook, Paul Harrison, Michael Lydeamore, and Thiyanga S. Talagala

**Abstract** A high-dimensional dataset is one where each observation is described by many features, or dimensions, with associations between them. These datasets contain nonlinear manifolds in image and speech recognition, clusters in genomics and forensic analysis, and sparse distributions in text mining. We can generate data containing a variety of structures using mathematical functions and statistical distributions. High-dimensional data structures are useful for testing, validating, and improving algorithms used in dimensionality reduction, clustering, machine learning, and visualization. Their controlled complexity allows researchers to understand challenges posed in data analysis and helps to develop robust analytical methods across diverse scientific fields like bioinformatics, machine learning, and forensic science. Functions to generate a large variety of structures in high dimensions are organized into the R package `cardinalR`, along with some already generated examples, adding to the existing toolset of benchmark datasets for evaluating algorithms.

## 1 Introduction

Generating synthetic datasets with clearly defined geometric properties is useful for evaluating and benchmarking algorithms in various fields, such as machine learning, data mining, and computational biology. Researchers often need to generate data with specific dimensions, noise characteristics, and complex underlying structures to test the performance and robustness of their methods.

There are numerous packages available in R for generating synthetic data, each designed with unique characteristics and focus areas. The `geozoo` package ([Schloerke \(2016\)](#)) offers a large collection of geometric objects, allowing users to create and analyze specific shapes, primarily in lower-dimensional spaces. Another useful package is `snpdata` ([Melville \(2025\)](#)), which provides tools for generating simplified datasets useful for evaluating dimensionality reduction techniques like tSNE, often focusing on understanding and evaluating low-dimensional embeddings of complex data structures. Additionally, `mlbench` ([Leisch and Dimitriadou \(2024\)](#)) includes a collection of well-known benchmark datasets commonly associated with established classification or regression challenges. In the field of single-cell omics, `splatter` ([Zappia et al. \(2017\)](#)) is designed to simulate complex biological data, capturing field-specific nuances such as batch effects and differential expression. While these packages are valuable, their scope is often limited to specific applications or low-dimensional structures.

To address this gap, this paper introduces the `cardinalR` R package. This package provides a collection of functions designed to generate customizable data structures in any number of dimensions, starting from basic geometric shapes. `cardinalR` offers important functionalities that extend beyond the capabilities of existing tools, allowing users to: (i) construct high-dimensional datasets based on geometric shapes, including the option to enhance dimensionality by adding controlled noise dimensions; (ii) introduce adjustable levels of background noise to these structures; and (iii) combine high-dimensional datasets into a single multi-faceted, clustered dataset in a space of arbitrary dimension. By using clearly defined geometric shapes and controllable characteristics such as number of dimensions, sample size; `cardinalR` allows researchers to generate transparent and interpretable synthetic datasets for evaluating algorithm performance in high-dimensional settings.

By providing these aspects, `cardinalR` provides researchers with a method to generate more explainable and challenging high-dimensional clustering synthetic datasets focused to the specific needs of evaluating algorithms.

The paper is organized as follows. In the next section, we introduce the implementation of the `cardinalR` package on GitHub, including a demonstration of the package's key functions. We illustrate how a clustering data structure affects the dimension reductions in the Application section. Finally, we give a brief conclusion of the paper and discuss potential opportunities for the use of our data collection.

## 2 Implementation

### Installation

The development version can be installed from GitHub:

**Table 1:** The main arguments for gen\_multiclus().

| Argument | Type               | Explanation  |
|----------|--------------------|--|
| n        | numeric (vector)   | Number of points in each cluster.                                    |
| p        | numeric            | Number of dimensions.  |
| k        | numeric            | Number of clusters.  |
| loc      | numeric (matrix)   | Locations/centroids of clusters.                                     |
| scale    | numeric (vector)   | Scaling factors of clusters.   |
| shape    | character (vector) | Shapes of clusters.  |
| rotation | numeric (list)     | Plane and the corresponding angle along that plane for each cluster. |
| is_bkg   | boolean            | Background noise should exist or not.                                |

```
pak::pak("JayaniLakshika/cardinalR")
```

## Usage

### Main function

The main function of the package is `gen_multiclus()`, which generates datasets consisting of multiple clusters with user-specified characteristics. Users can control the number of clusters (`k`), the number of points in each cluster (`n`), and the dimensionality of the space (`p`) for all the clusters. Each cluster can take on a different geometric shape (e.g., Gaussian, cone, uniform cube) by specifying the corresponding generator function (`shape`), can be scaled to adjust its spread, rotated in specified planes by given angles, and positioned at defined centroids (`loc`). The function ensures flexibility in cluster location and orientation, allowing users to simulate complex high-dimensional structures. An optional argument, `is_bkg`, adds background noise drawn from a multivariate normal distribution centered on the dataset's overall mean with standard deviations matching the observed spread. Extra arguments (...) can be passed to cluster generators, allowing further control over per-cluster characteristics such as noise structure.

The main arguments of the `gen_multiclus()` function are shown in Table 1.

### Shape generators

The shape generators form the foundation of the package, providing a collection of functions to create synthetic data structures based on simple, well-defined geometric structures. These include fundamental shapes such as cones, pyramids, spheres, grids, and branching structures. If a shape is not inherently defined in more than three dimensions, additional noise dimensions can be added to embed the structure into higher-dimensional space. Users can specify how these noise dimensions are generated (e.g., Gaussian, wavy) (`noise_fun`), offering control over the embedding process. All shape generators allow the user to define the number of points (`n`) and dimensions (`p`), and most include additional arguments to customize specific characteristics of the structure.

**Branching** A branching structure (Figure 1) captures trajectories that diverge or bifurcate from a common origin, similar to processes such as cell differentiation in biology (Trapnell et al. (2014)). We introduce a set of data generation functions specifically designed to simulate high-dimensional branching structures with various geometries, numbers of points (`n`), and number of branches (`k`). Although these functions can generate multiple branches, they do not produce a formal *multiclus* dataset: the branches form a single connected structure, with multiple visually distinct arms rather than independent clusters. Table 2 outlines these functions. The main arguments of the functions described in Table 3.

The simplest structures are approximately linear branches, generated by the `gen_linearbranches(n, p, k)` function (Figure 1 b). These consist of  $k$  short line segments in the first two dimensions, with added jitter to simulate variability. Mathematically, each branch  $i$  is defined as

$$X_1 \sim U(a_i, b_i), \quad X_2 = s_i(X_1 - x_{\text{start},i}) + y_{\text{start},i} + \epsilon, \quad \epsilon \sim U(0, \delta),$$

where  $(x_{\text{start},i}, y_{\text{start},i})$  is the starting point of branch  $i$ ,  $\delta$  controls local jitter, and  $s_i$  is the slope, initialized as

**Table 2:** cardinalR branching data generation functions

| Function              | Explanation                                     |
|-----------------------|---|
| gen_expbranches       | Exponential shaped branches.                    |
| gen_linearbranches    | Linear shaped branches.                         |
| gen_curvybranches     | Curvy shaped branches.                          |
| gen_orglinearbranches | Linear shaped branches originated in one point. |
| gen_orgcurvybranches  | Curvy shaped branches originated in one point.  |

**Table 3:** The main arguments for branching shape generators.

| Argument | Explanation  |
|----------|--|
| n        | A numeric value representing the number of points.     |
| p        | A numeric value representing the number of dimensions. |
| k        | A numeric value representing the number of clusters.   |

$$s_i = \begin{cases} 0.5 & i = 1, \\ -0.5 & i = 2, \\ \text{randomly sampled from } [s_{\min}, s_{\max}] & i = 3, \dots, k. \end{cases}$$

Branches 1 and 2 are initialized with fixed slopes and intercepts, while later branches are iteratively added at locations chosen to avoid overlap with existing branches, producing a set of connected linear paths.

```
linearbranches <- gen_linearbranches(n = 1000, p = 4, k = 4)
```

To introduce curvature, the `gen_curvybranches(n, p, k)` function generates  $k$  curvilinear branches in  $p$ -D (Figure 1 c). Branches 1 and 2 are simple parabolas defined as

$$\begin{aligned} \text{Branch 1: } X_1 &\sim U(0, 1), \quad X_2 = 0.1X_1 + X_1^2 + \epsilon, \\ \text{Branch 2: } X_1 &\sim U(-1, 0), \quad X_2 = 0.1X_1 - 2X_1^2 + \epsilon, \quad \epsilon \sim U(0, \delta), \end{aligned}$$

where  $\delta$  controls local jitter. Additional branches are attached iteratively to existing structures. Each new branch  $i$  starts at a selected point  $(x_{\text{start},i}, y_{\text{start},i})$  from the current structure and extends according to

$$X_1 \sim U(x_{\text{start},i}, x_{\text{start},i} + 1), \quad X_2 = 0.1X_1 - s_i(X_1^2 - x_{\text{start},i}) + y_{\text{start},i},$$

where  $s_i$  is a scale factor controlling the curvature of branch  $i$ . For the first few initial branches,  $s_i$  can be fixed (e.g.,  $s_1 = 1, s_2 = 2$ ), while for subsequent branches it is sampled from a predefined set, such as  $s_i \in \{-2, -1.5, -1, -0.5, 0, 0.5, 1, 1.5\}$ , to create variability in curvature.

```
curvybranches <- gen_curvybranches(n = 1000, p = 4, k = 4)
```

The `gen_expbranches(n, p, k)` function creates  $k$  exponential branches in 2-D, radiating from a central region (Figure 1 a). Each branch  $i$  is defined as

$$X_1 \sim U(-2, 2), \quad X_2 = \exp(\sigma_i s_i X_1) + \epsilon, \quad \epsilon \sim U(0, \delta), \quad s_i \sim U(0.5, 2),$$

where  $\sigma_i = (-1)^{i+1}$  alternates the sign of the exponent to produce mirror-symmetric branches. The parameter  $s_i$  controls the steepness of branch  $i$ , and  $\delta$  introduces small local jitter.

```
expbranches <- gen_expbranches(n = 1000, p = 4, k = 4)
```

High-dimensional generalizations are provided by `gen_orglinearbranches(n, p, k)` and `gen_orgcurvybranches(n, p, k)` (Figure 1 d-e). Each branch is embedded in a unique or repeated 2-D subspace of the  $p$ -D space. When `allow_share = TRUE`, multiple branches may share the same subspace; otherwise, subspaces are

sampled without replacement until all possible  $\binom{p}{2}$  combinations are exhausted, after which additional branches may repeat subspaces. Linear branches follow

$$X_{i_1} \sim U(a_i, b_i), \quad X_{i_2} = s_i X_{i_1} + \epsilon, \quad \epsilon \sim N(0, \sigma^2),$$

while curvilinear branches include a quadratic term

$$X_{i_1} \sim U(a_i, b_i), \quad X_{i_2} = -s_i X_{i_1}^2 + \epsilon, \quad \epsilon \sim N(0, \sigma^2),$$

where  $a_i, b_i$  define the range of the first coordinate for branch  $i$ , and  $\epsilon$  is Gaussian noise added to introduce variability. The scale factor  $s_i$  controls slope (linear branches) or curvature (curvilinear branches) and is assigned as follows: for the first  $\binom{p}{2}$  branches,  $s_i = 1$ ; for additional branches when  $k > \binom{p}{2}$ ,  $s_i$  is randomly drawn from the set  $\{1, 1.5, 2, \dots, 8\}$ .

```
orglinearbranches <- gen_orglinearbranches(n = 1000, p = 4, k = 4)
```

```
orgcurvybranches <- gen_orgcurvybranches(n = 1000, p = 4, k = 4)
```

For all branch-generating functions, when the target dimensionality  $p > 2$ , additional dimensions are filled with independent noise, allowing the 2-D or 2-D-subspace structures to be naturally embedded in higher-dimensional space while preserving the intended geometric patterns.

**Cone** To simulate a cone-shaped structure in arbitrary dimensions (Figure 2), we define a function `gen_cone(n, p, h, ratio)`, which creates a high-dimensional cone with options for a sharp or blunted apex, allowing for a dense concentration of points near the tip.

This function generates  $n$  points in  $p$ -D, where the last dimension,  $X_p$ , represents the height along the cone's axis, and the first  $p - 1$  dimensions define a shrinking hyperspherical cross-section toward the tip. Heights are sampled from a truncated exponential distribution,  $X_p \sim \text{Exp}(\lambda = 2/h)$ , capped at the cone height  $h$ , producing a higher density of points near the tip. At each height  $X_p$ , the radius of the cross-section decreases linearly from base to tip according to  $r = r_{\min} + (r_{\max} - r_{\min})X_p/h$ , where  $r_{\min} = \text{ratio}$  and  $r_{\max} = 1$ .

For each point, a direction in the first  $p - 1$  dimensions is sampled uniformly on a  $(p - 1)$ -dimensional hypersphere using generalized spherical coordinates. The radial coordinates are scaled by the height-dependent radius  $r$ , producing the conical taper. In three dimensions ( $p = 3$ ), this results in a classical 3-D cone, while for  $p > 3$ , additional dimensions provide a smooth embedding into higher-dimensional space, preserving the conical structure.

```
cone <- gen_cone(n = 1000, p = 4, h = 5, ratio = 0.5)
```

**Cube** A cube structure (Figure 3) represents uniformly or systematically distributed points within a high-dimensional hypercube, providing a useful framework for assessing how well algorithms preserve uniformity, spacing, and boundary properties in high dimensions. We provide a set of functions to generate high-dimensional cube structures with flexible configurations, including regular grids, uniform random points, and cubes with missing regions or holes. These structures are valuable for testing the ability of algorithms to maintain uniform spacing or to detect gaps in the data. Table 4 outlines these functions and their purposes.

The first is the regular grid of points of  $n$  points in  $p$  dimensions. This is generated using `gen_gridcube(n, p)`. The number of grid points along each axis is determined by finding the nearest integer factors whose product is close to  $n$ . Each dimension is then normalized to lie in the interval  $[0, 1]$ , so that the resulting structure forms a true  $p$ -D hypercube. This produces a lattice of evenly spaced points along all axes, providing a uniform and interpretable high-dimensional grid.

```
gridcube <- gen_gridcube(n = 1000, p = 4)
```

An extension to the regular grid of points is to consider the points being uniformly distributed along each axis, as opposed to evenly spaced. The function `gen_unifcube(n, p)` is identical to the regular grid of points, except instead of points being placed in integer grid coordinates, they are placed at a uniformly distributed point inside the  $p$ -D cube (Figure 3 b).

```
unifcube <- gen_unifcube(n = 1000, p = 4)
```

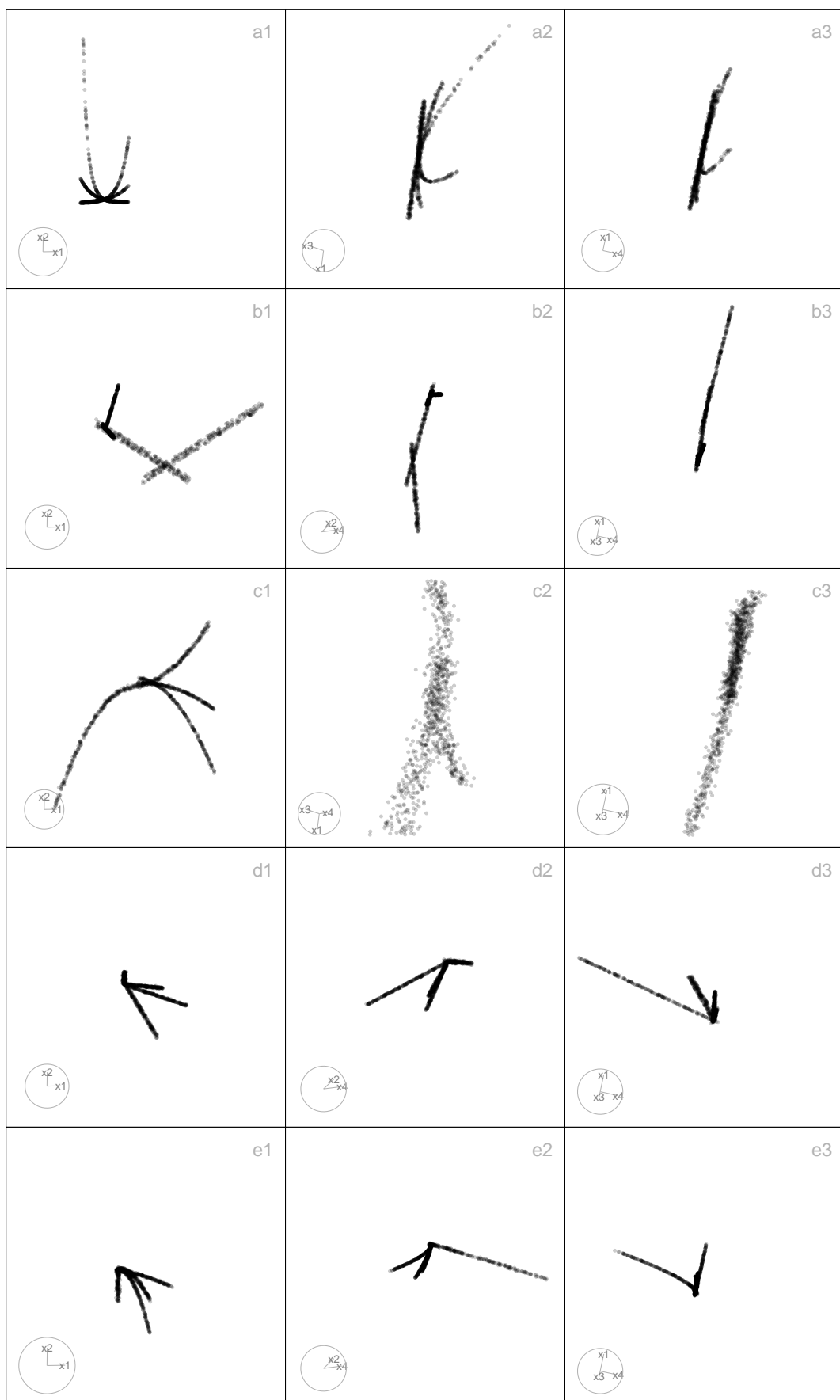


**Figure 1:** Three 2-D projections from 4-D, for the ‘expbranches’ (a1-a3), ‘linearbranches’ (b1-b3), ‘curvybranches’ (c1-c3), ‘orglinearbranches’ (d1-d3), ‘orgcurvybranches’ (e1-e3) data.

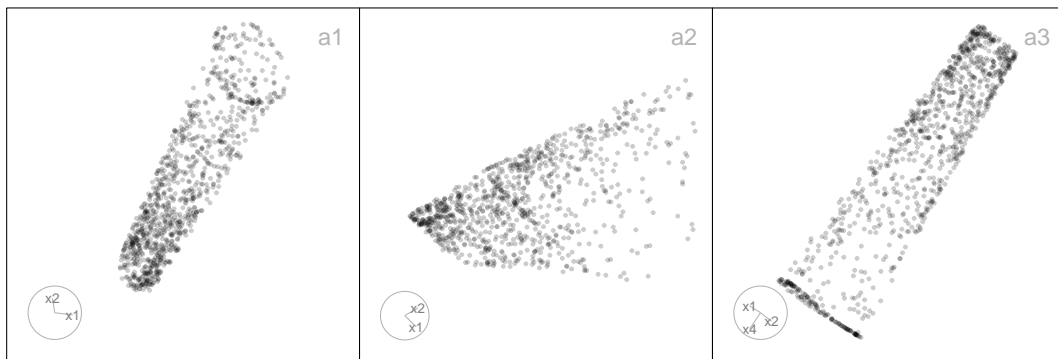


**Figure 2:** Three 2-D projections from 4-D, for the ‘cone’ data.

**Table 4:** cardinalR cube data generation functions

| Function     | Explanation                                      |
|--------------|--|
| gen_gridcube | Cube with specified grid points along each axes. |
| gen_unifcube | Cube with uniform points.                        |
| gen_cubehole | Cube with a hole.                                |

Finally, we consider a cube that has a central spherical hole. This is generated using the `gen_cubehole(n, p, r_hole)` function. The cube is generated as per the uniformly distributed cube, but points inside sphere of radius (`r_hole`) are removed, resulting in a hollow cube structure (Figure 3 c).

```
cubehole <- gen_cubehole(n = 3000, p = 4, r_hole = 0.5)
```

**Gaussian** The `gen_gaussian(n, p, s)` function generates a multivariate Gaussian cloud in  $p$ -D, centered at the origin with user-defined covariance structure (Figure 4). Each point is independently drawn using the multivariate normal distribution with  $X_i \sim N_p(\mathbf{0}, s)$ , where  $s$  is a user-defined  $p \times p$  positive-definite matrix.

```
gau <- gen_gaussian(n = 1000, p = 4, s = diag(4))
```

**Linear** The `gen_longlinear(n, p)` function generates a high-dimensional dataset representing a long linear structure with noise. Each variable is formed as  $X_i = \text{scale}_i \cdot (0, 1, \dots, n-1 + \epsilon) + \text{shift}_i$ , where  $\text{scale}_i \sim U(-10, 10)$  determines the orientation of the line in each dimension,  $\text{shift}_i \sim U(-300, 300)$  offsets the line to separate dimensions, and  $\epsilon \sim N(0, (0.03n)^2)$  introduces Gaussian noise.

```
linear <- gen_longlinear(n = 1000, p = 4)
```

**Mobius** The `gen_mobius(n, p)` function generates a dataset of  $n$  points that form a Möbius strip embedded in the first three dimensions of a  $p$ -D structure (Figure 6). This classical non-orientable surface loops back on itself with a half-twist.

The Möbius strip is generated using the `geozoo::mobius` function with  $p = 3$ , and  $n$  defined as above. Each point is sampled from a parameterization defined by an angle  $\theta \sim U(0, 2\pi)$ , which specifies the position along the circular loop, and a width  $w \sim U(-0.4, 0.4)$ , which offsets the point across the strip’s band. The cartesian coordinates are

$$X_1 = (1 + (w/2) \cos(\theta/2)) \cos(\theta), \quad X_2 = (1 + (w/2) \cos(\theta/2)) \sin(\theta), \text{ and } X_3 = (w/2) \sin(\theta/2).$$

This maps a 2-D band with a half-twist into 3-D space, forming a non-orientable one-sided surface. For  $p > 3$ , additional noise dimension are added to embed the 3-D Möbius into  $p$ -D.

```
mobius <- gen_mobius(n = 1000, p = 4)
```

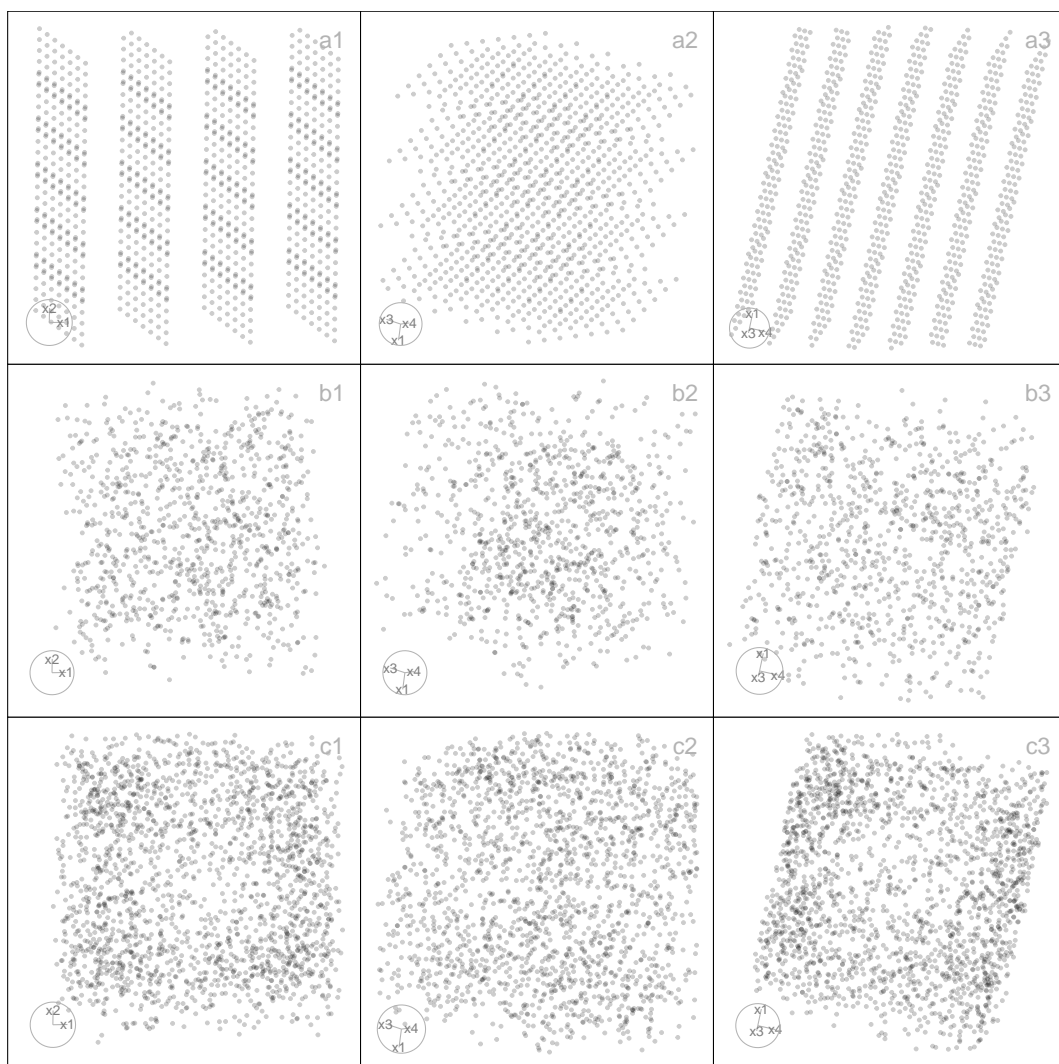


**Figure 3:** Three 2-D projections from 4-D, for the ‘gridcube’ (a1-a3), ‘unifcube’ (b1-b3), and ‘cubehole’ (c1-c3) data.

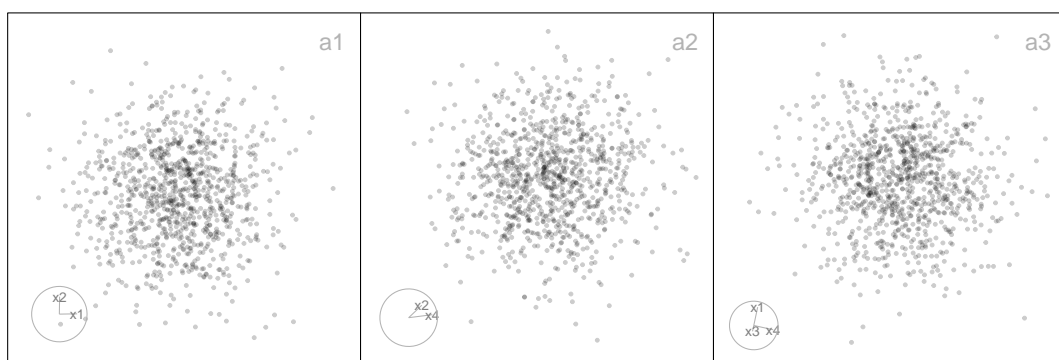


**Figure 4:** Three 2-D projections from 4-D, for the ‘gau’ data.

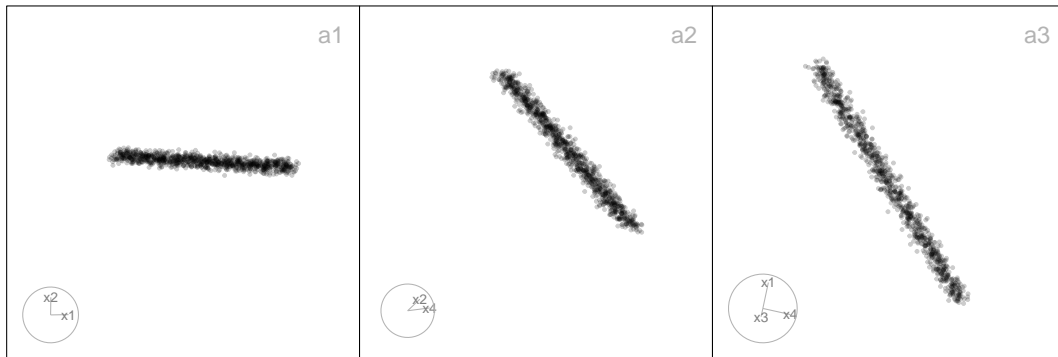


**Figure 5:** Three 2-D projections from 4-D, for the ‘linear’ data.

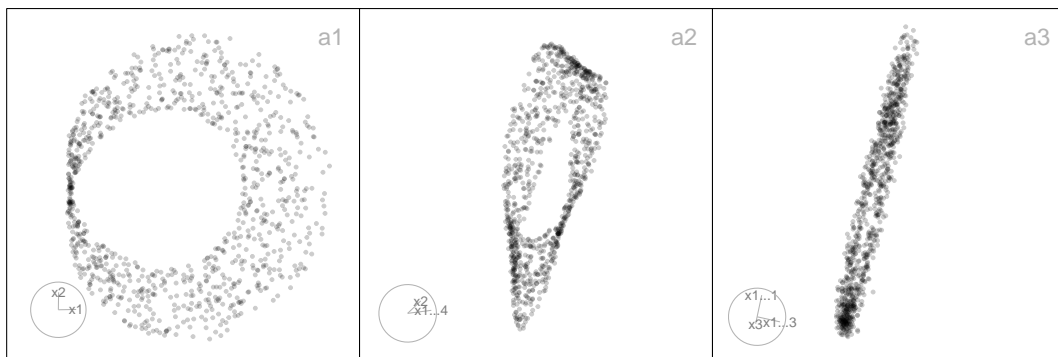


**Figure 6:** Three 2-D projections from 4-D, for the ‘mobius’ data.

**Polynomial** A polynomial structure (Figure 7) generates data points that follow non-linear curvilinear relationships, such as quadratic or cubic trends, in high-dimensional space. These patterns are useful for evaluating how well algorithms capture smooth, non-linear trajectories and curvature in the data. We provide functions for generating quadratic and cubic structures, enabling controlled experiments with different degrees of polynomial complexity. Table 5 summarizes these functions and their purposes.

The first is the quadratic curve of  $n$  points in  $p$  dimensions. This is generated using `gen_quadratic(n, p, range)`. The independent variable is defined as  $X_1 \sim U(\text{range}[1], \text{range}[2])$ , and a raw polynomial basis of degree 2 is applied to form  $X_2 = X_1 - X_1^2 + \epsilon_2$ , where  $\epsilon_2 \sim U(0, 0.5)$ . This produces a smooth parabolic arc opening downward, with vertical jitter introduced by the noise term (Figure 7 a).

```
quadratic <- gen_quadratic(n = 1000, p = 4)
```

The second is the cubic curve of  $n$  points in  $p$  dimensions. This is generated using `gen_cubic(n, p, range)`. The independent variable is defined as  $X_1 \sim U(\text{range}[1], \text{range}[2])$ , and a raw polynomial basis of degree 3 is applied to construct  $X_2 = X_1 + X_1^2 - X_1^3 + \epsilon_2$ , where  $\epsilon_2 \sim U(0, 0.5)$ . This produces a more complex curvilinear structure than the quadratic case, with both upward and downward turning points (Figure 7 b).

```
cubic <- gen_cubic(n = 1000, p = 4)
```

For all polynomial shapes, if  $p > 2$ , the structure is embedded into higher dimensions by appending additional noise dimensions.

**Table 5:** cardinalR polynomial data generation functions

| Function                   | Explanation        |
|----------------------------|--------------------|
| <code>gen_quadratic</code> | Quadratic pattern. |
| <code>gen_cubic</code>     | Cubic pattern.     |

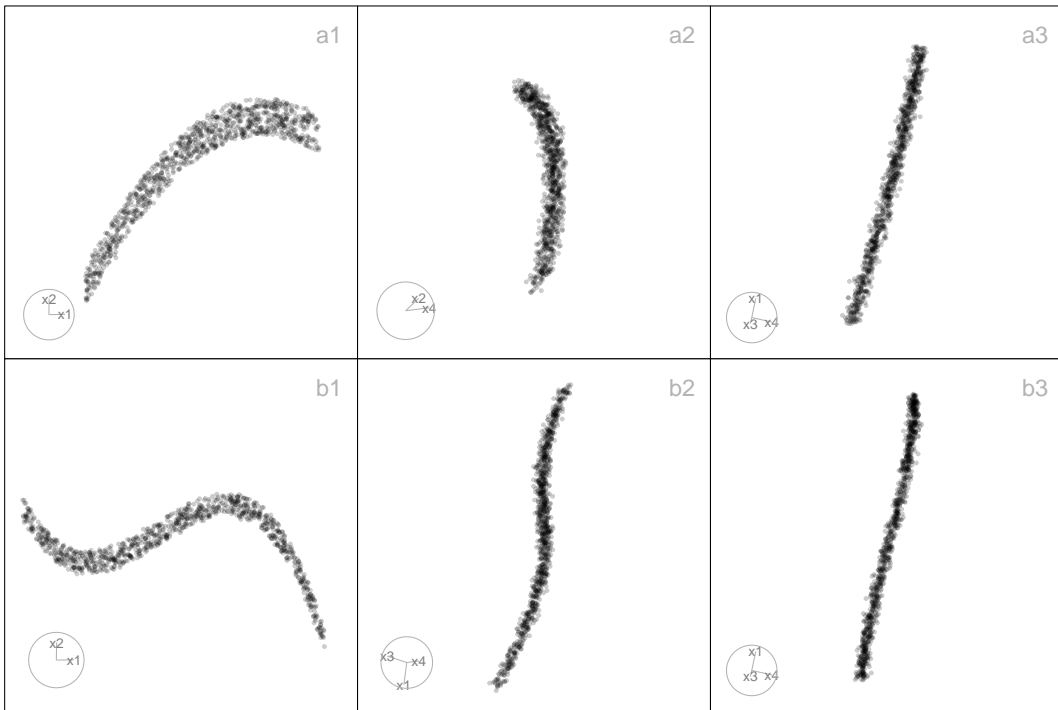


**Figure 7:** Three 2-D projections from 4-D, for the ‘quadratic’ (a1-a3) and ‘cubic’ (b1-b3) data.

**Pyramid** A pyramid structure (Figure 8) represents data arranged around a central apex and base, useful for exploring how algorithms handle pointed or layered geometries in high-dimensional space. The functions provided allow users to generate pyramids with rectangular, triangular, and star-shaped bases, and sharp or blunted apexes. Additionally, it is possible to create a pyramid with a fractal-like internal structure, enabling the study of non-convex and sparse regions. Table 6 summarizes these functions.

Let  $X_1, \dots, X_p$  denote the coordinates of the generated points. For the rectangular and triangular based pyramid generator functions, the final dimension,  $X_p$ , encodes the height of each point and is drawn from an exponential distribution capped at the maximum height  $h$ . That is,

$$X_p = z \sim \min(\text{Exp}(\lambda = 2/h), h).$$

This distribution creates a natural skew toward smaller height values, resulting in a denser concentration of points near the pyramid’s apex. For the star-shaped base pyramid, the final dimension is drawn from a uniform distribution. That is,  $X_p = z \sim U(0, h)$ .

The remaining dimensions are based on the specific pyramid shape. For the rectangular based pyramid, `gen_pyrrect(n, p, h, l_vec, rt)` (Figure 8 a), let  $r_x(z)$  and  $r_y(z)$  denote the half-widths of the rectangular cross-section at height  $z$ . That is,  $r_x(z) = r_t + (l_x - r_t)z/h$ ,  $r_y(z) = r_t + (l_y - r_t)z/h$ . The first three coordinates are then defined as:

$$X_1 \sim U(-r_x(z), r_x(z)), \quad X_2 \sim U(-r_y(z), r_y(z)), \text{ and } X_3 \sim U(-r_x(z), r_x(z)).$$

```
pyrrect <- gen_pyrrect(n = 1000, p = 4)
```

For the triangular based pyramid, `gen_pyrtri(n, p, h, l, rt)` (Figure 8 b), let  $r(z)$  denote the scaling factor (distance from the origin to triangle vertices) at height  $z$ . That is,  $r(z) = r_t + (l - r_t)z/h$ . A point in the triangle at height  $z$  is generated using barycentric coordinates  $(u, v)$  to ensure uniform sampling within the triangular cross-section:  $u, v \sim U(0, 1)$ , if  $u + v > 1$ :  $u \leftarrow 1 - u$ ,  $v \leftarrow 1 - v$ . The first three coordinates (triangle plane) are then:  $X_1 = r(z)(1 - u - v)$ ,  $X_2 = r(z)u$ , and  $X_3 = r(z)v$ .

```
pyrtri <- gen_pyrtri(n = 1000, p = 4)
```

For the star based pyramid, `gen_pyrstar(n, p, h, rb)` (Figure 8 c), let the radius at height  $z$ ,  $r(z)$ , be such that the radius scales linearly from zero (tip) to the base radius  $r_b$ . That is,  $r(z) = r_b(1 - z/h)$ .

Each point is placed within a regular hexagon in the plane  $(X_1, X_2)$ , using a randomly chosen hexagon sector angle  $\theta \in \{0, \pi/3, 2\pi/3, \pi, 4\pi/3, 5\pi/3\}$  and a uniformly random radial scaling factor:

**Table 6:** cardinalR pyramid data generation functions

| Function    | Explanation   |
|-------------|---|
| gen_pyrrect | Rectangular-base pyramid, with a sharp or blunted apex. |
| gen_pyrtri  | Triangular-base pyramid, with a sharp or blunted apex.  |
| gen_pyrstar | Star-shaped base pyramid, with a sharp or blunted apex. |
| gen_pyrfrac | Pyramid containing triangular pyramid-shaped holes.     |

**Table 7:** cardinalR S-curve data generation functions

| Function       | Explanation          |
|----------------|----------------------|
| gen_scurve     | S-curve.             |
| gen_scurvehole | S-curve with a hole. |

$\theta \sim$  Uniform sample from 6 hexagon angles,  $r_{\text{point}} \sim \sqrt{U(0,1)}$ . Then, the first two coordinates are:  $X_1 = r(z)r_{\text{point}} \cos(\theta)$ , and  $X_2 = r(z)r_{\text{point}} \sin(\theta)$ .

```
pyrstar <- gen_pyrstar(n = 1000, p = 4)
```

For all the above pyramid shapes, if  $p > 3$ , the remaining  $p - 3$  dimensions (i.e.,  $X_4$  to  $X_{p-1}$ ) are additional noise.

Finally, for the Sierpinski-like pyramid,  $\text{gen\_pyrfrac}(n, p)$  (Figure 8 d), let  $X_1, X_2, \dots, X_p$  denote the coordinates of the generated points. The generation process begins with an initial point  $T_0 \in [0, 1]^p$  drawn from a uniform distribution:  $T_0 \sim U(0, 1)^p$ . Let  $C_1, C_2, \dots, C_{p+1}$  denote the corner vertices of a  $p$ -D simplex. At each iteration  $i = 1, \dots, n$ , a new point is computed by taking the midpoint between the previous point  $T_{i-1}$  and a randomly selected vertex  $C_k$ :  $T_i = 1/2(T_{i-1} + C_k)$ ,  $C_k \in \{C_1, \dots, C_{p+1}\}$ . This recursive midpoint rule generates self-similar patterns with systematic voids (holes) between clusters of points. The points remain bounded inside the convex hull of the simplex. The final output is a  $n \times p$  matrix where each row represents a point:  $X = \{T_1, T_2, \dots, T_n\}$ ,  $X \in \mathbb{R}^{n \times p}$ .

```
pyrholes <- gen_pyrfrac(n = 1000, p = 4)
```

**S-curve** An S-curve structure (Figure 9) simulates data that lies along a smooth, non-linear manifold. The functions generate both the standard S-curve shape and, a S-curve variant with structured hole that introduce missing or incomplete region. These variations are useful for evaluating how well algorithms capture non-linear geometry and handle incomplete manifolds in high-dimensional data. Table 7 summarizes these functions.

For the S-curve structure,  $\text{gen\_scurve}(n, p)$  (Figure 9 a), the 3-D geometry is constructed by introducing a latent parameter,  $\theta \sim U(-3\pi/2, 3\pi/2)$ . This parameter controls the curvature of the manifold. The first three dimensions form the S-curve structure:

$$X_1 = \sin(\theta), \quad X_2 \sim U(0, 2), \quad X_3 = \text{sign}(\theta)(\cos(\theta) - 1)$$

. This configuration creates a horizontally curled shape in  $(X_1, X_3)$ , with additional band thickness in the  $X_2$  direction. For  $p > 3$ , additional noise dimensions are appended to embed the structure in higher dimensions.

```
scurve <- gen_scurve(n = 1000, p = 4)
```

To introduce missing or incomplete regions on the manifold,  $\text{gen\_scurvehole}(n, p)$  (Figure 9 b) removes points in a localized region centered around the middle vertical section of the S-curve. Following a similar approach as  $\text{gen\_cubehole}()$ , all observations within a fixed radius ( $\sqrt{0.3}$ ) of the anchor point are excluded, creating a hole in the manifold while preserving the overall S-curve structure.

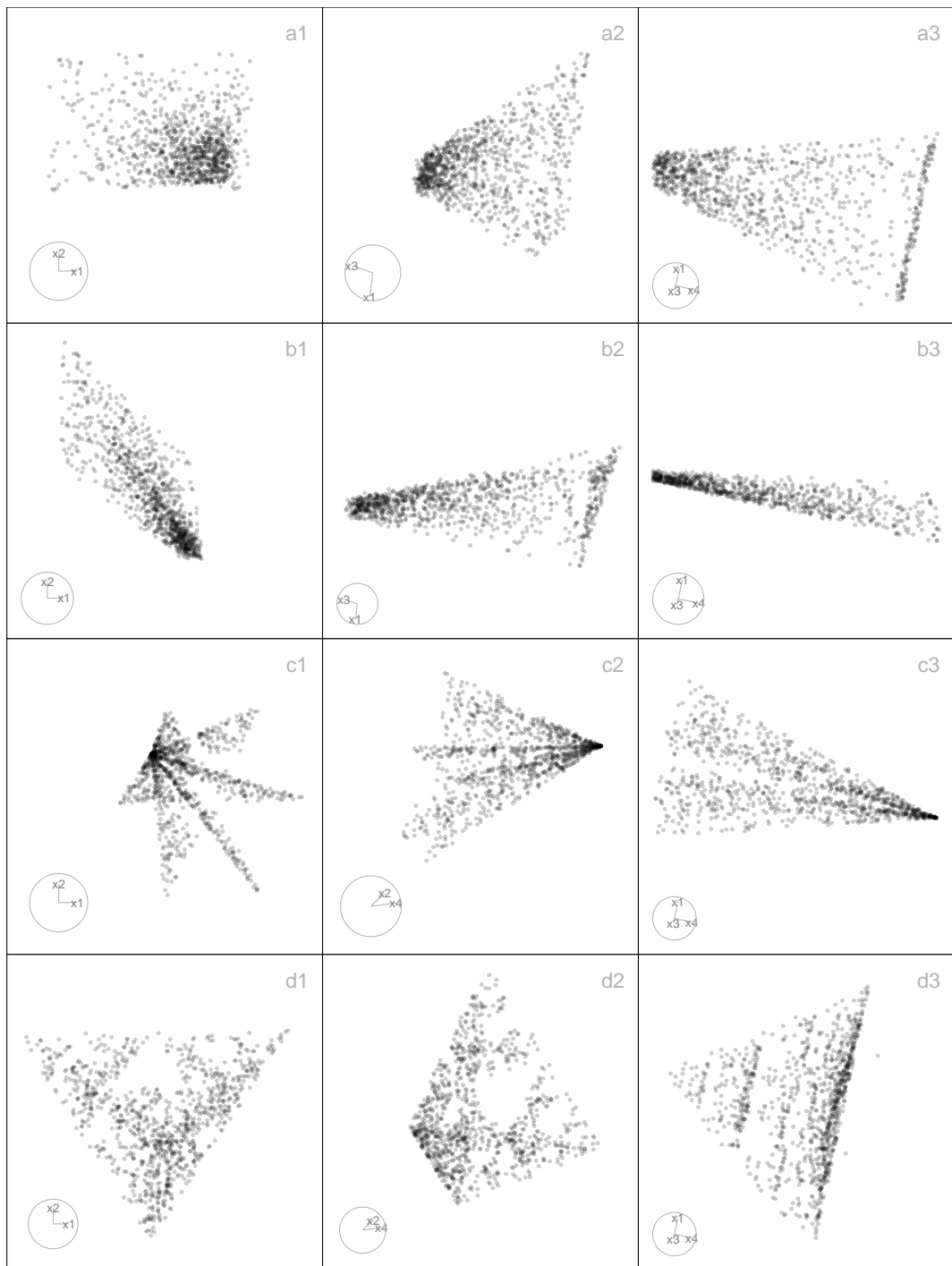


**Figure 8:** Three 2-D projections from 4-D, for the ‘pyrrect’ (a1-a3), ‘pyrtri’ (b1-b3), ‘pyrstar’ (c1-c3), and ‘pyrholes’ (d1-d3) data.

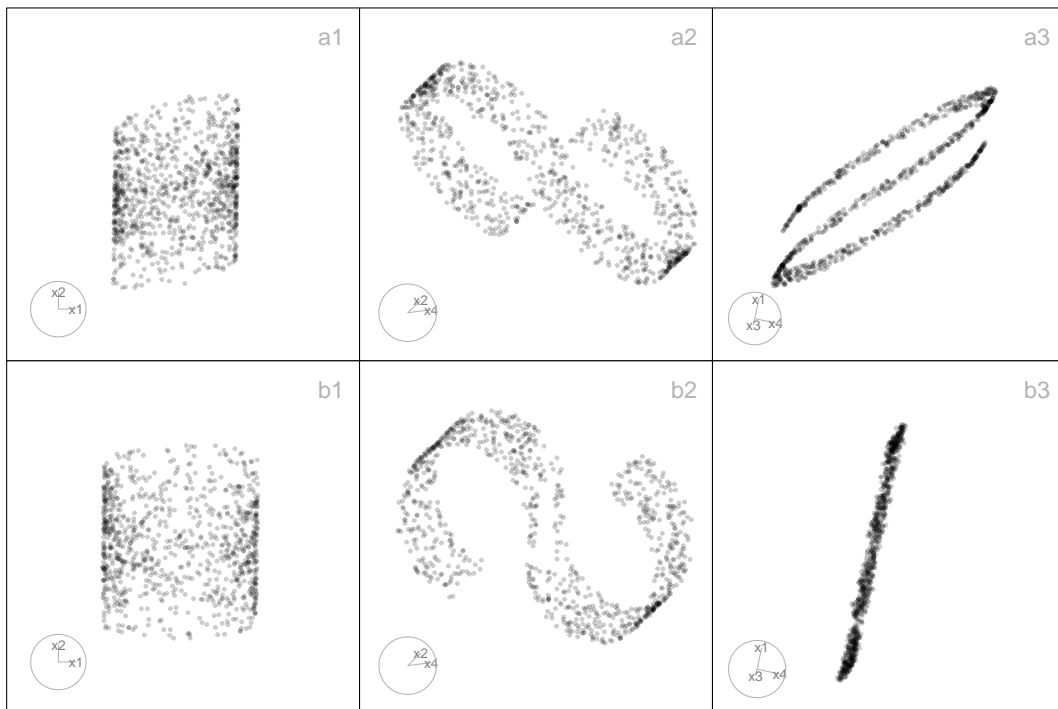


**Figure 9:** Three 2-D projections from 4-D, for the ‘scurve’ (a1-a3) and ‘scurvehole’ (b1-b3) data.

**Table 8:** cardinalR sphere data generation functions

| Function             | Explanation                                 |
|----------------------|---|
| gen_circle           | Circle.                                     |
| gen_curvycycle       | Curvy cell cycle.                           |
| gen_unifsphere       | Uniform sphere.                             |
| gen_griddedsphere    | Gridded sphere.                             |
| gen_clusteredspheres | Multiple small spheres within a big sphere. |
| gen_hemisphere       | Hemisphere.                                 |

```
scurvehole <- gen_scurvehole(n = 1000, p = 4)
```

**Sphere** Sphere-shaped structures (Figure 10) are useful for evaluating how dimension reduction and clustering algorithms handle curved, symmetric manifolds in high-dimensional spaces. The functions generate a variety of spherical forms, including simple circles, uniform spheres, grid-based spheres, and complex arrangements like clustered spheres within a larger sphere. The first few coordinates define the main geometric form (circle, cycle, sphere, or hemisphere), while higher-dimensional embeddings are achieved by adding noise dimensions. For the circle and curvy cycle, this occurs when  $p > 2$  and  $p > 3$ , respectively, while for spheres and hemispheres it occurs when  $p > 3$  or  $p > 4$ . Table 8 summarizes these functions.

The simplest case, `gen_circle(n, p)` creates a unit circle in two dimensions, with the remaining dimensions forming sinusoidal extensions of the angular parameter at progressively smaller scales (Figure 10 a). Let a latent angle variable  $\theta$  is uniformly sampled from the interval  $[0, 2\pi]$ . Coordinates in the first two dimensions represent a perfect circle on the plane:

$$X_1 = \cos(\theta), \quad X_2 = \sin(\theta)$$

. For dimensions  $X_3$  through  $X_p$ , sinusoidal transformations of the angle  $\theta$  are introduced. The first component is a scaling factor that decreases with the dimension index, defined as  $\text{scale}_j = \sqrt{(0.5)^{j-2}}$  for  $j = 3, \dots, p$ . The second component is a phase shift that is proportional to the dimension index, specifically designed to decorrelate the curves, given by the formula  $\phi_j = (j-2)\pi/2p$ . Each additional dimension is computed as:  $X_j = \text{scale}_j \sin(\theta + \phi_j), \quad j = 3, \dots, p$ .

```
circle <- gen_circle(n = 1000, p = 4)
```

For the one-dimensional nonlinear cycle embedded in  $p$ -D space, `gen_curvycycle(n, p)` (Figure 10 b), let a latent angle variable  $\theta$  is uniformly sampled from the interval  $[0, 2\pi]$ . The first three dimensions define a non-circular closed curve, referred to as a “curvy cycle”. In this configuration,  $X_1 = \cos(\theta)$  represents horizontal oscillation, while  $X_2 = \sqrt{3}/3 + \sin(\theta)$  introduces a vertical offset to avoid centering the curve at the origin. Additionally,  $X_3 = 1/3 \cos(3\theta)$  introduces a third harmonic perturbation that intricately folds the curve three times along its path, creating a unique and complex shape that oscillates in both dimensions while incorporating the effects of the harmonic perturbation.

Together, these define a periodic, non-trivial, closed curve in 3-D with internal folds that produce a more complex geometry than a standard circle or ellipse. For dimensions  $X_4$  through  $X_p$ , additional structured variability is introduced through decreasing amplitude scaling and phase-shifted sine waves. The scaling factor is defined as  $\text{scale}_j = \sqrt{(0.5)^{j-3}}$  for  $j$  ranging from 4 to  $p$ , which means that the amplitude decreases as the dimension increases. Each dimension  $X_j$  is then calculated using the formula  $X_j = \text{scale}_j \sin(\theta + \phi_j)$ , where the phase shift  $\phi_j$  is given by  $\phi_j = (j - 2)\pi/2p$ .

```
curvycycle <- gen_curvycycle(n = 1000, p = 4)
```

Building on simple circular structures, the `gen_unifsphere(n, p, r)` function extends the idea to three dimensions by generating  $n$  observations approximately uniformly distributed on the surface of a sphere of radius  $r$ , with optional high-dimensional noise when  $p > 3$  (Figure 10 c). Each observation is computed from spherical coordinates, with  $u \sim U(-1, 1)$  representing  $\cos(\phi)$  and  $\theta \sim U(0, 2\pi)$  the azimuthal angle. Cartesian coordinates are then defined as

$$X_1 = r\sqrt{1 - u^2} \cos(\theta), \quad X_2 = r\sqrt{1 - u^2} \sin(\theta), \text{ and } X_3 = ru,$$

ensuring uniform distribution on the surface (not within) of the sphere. For  $p > 3$ , additional dimensions  $X_4$  through  $X_p$  are appended as structured noise.

```
unifsphere <- gen_unifsphere(n = 1000, p = 4)
```

In addition, the `gen_gridedsphere(n, p)` function constructs a  $p$ -D dataset consisting of approximately  $n$  points that are evenly distributed on the surface of the unit  $(p - 1)$ -sphere embedded in  $\mathbb{R}^p$  (Figure 10 d). The method relies on forming a regular grid in spherical coordinates, parameterized by  $(p - 1)$  angular variables: for dimensions  $j = 1, \dots, p - 2$  the polar angles are drawn from  $[0, \pi]$ , while the final angle ( $j = p - 1$ ) represents the azimuth and is drawn from  $[0, 2\pi]$ . The number of grid steps along each angular dimension is chosen by decomposing  $n$  into  $(p - 1)$  approximately equal integer factors using the helper function `gen_nproduct(n, p - 1)`.

Each grid point is subsequently mapped into Cartesian space via the standard hyperspherical-to-Cartesian transformation,

$$\begin{aligned} X_1 &= \cos(\theta_1), \\ X_2 &= \sin(\theta_1) \cos(\theta_2), \\ X_3 &= \sin(\theta_1) \sin(\theta_2) \cos(\theta_3), \\ &\vdots \\ X_{p-1} &= \sin(\theta_1) \sin(\theta_2) \cdots \sin(\theta_{p-2}) \cos(\theta_{p-1}), \\ X_p &= \sin(\theta_1) \sin(\theta_2) \cdots \sin(\theta_{p-2}) \sin(\theta_{p-1}). \end{aligned}$$

The result is a deterministic grid of points lying exactly on the surface of the unit  $(p - 1)$ -sphere, without any additional noise dimensions.

```
gridedsphere <- gen_gridedsphere(n = 1000, p = 4)
```

For more heterogeneous structures, the `gen_clusteredspheres(n, k, p, r, loc)` function generates one large sphere of radius  $r_1$  and  $k$  smaller spheres of radius  $r_2$ , each centered at a different random location (Figure 10 e). A large uniform sphere centered at the origin is created by sampling  $n_1$  points uniformly on the surface of a  $p$ -D sphere with a radius of  $r_1$ . The sampling is executed using the function `gen_unifsphere(n_1, p, r_1)`, which generates the desired points in the specified dimensional space. In generation of  $k$  smaller uniform spheres, each sphere contains  $n_2$  points that are sampled uniformly on a sphere with a radius of  $r_2$ . These spheres are positioned at distinct

random locations in  $p$ -space, with the center of each sphere being drawn from a normal distribution  $N(0, 1\text{oc}^2 I_p)$ . Points on spheres are generated using the standard hyperspherical method, which involves sampling  $u \sim U(-1, 1)$  to determine the cosine of the polar angle, and sampling  $\theta \sim U(0, 2\pi)$  to determine the azimuthal angle (for 3-D). Each observation is classified by cluster, with labels such as “big” for the large central sphere and “small\_1” to “small\_k” for the smaller spheres.

```
clusteredspheres <- gen_clusteredspheres(n = c(1000, 100), k = 3, p = 4, r = c(15, 3),
                                         loc = 10 / sqrt(3)) |>
  dplyr::select(-cluster)
```

Finally, the `gen_hemisphere(n, p)` function restricts sampling to a hemisphere of a 4-D sphere (Figure 10 f). Using spherical coordinates, the azimuthal angle  $\theta_1 \sim U(0, \pi)$  in the  $(x_1, x_2)$  plane, while the elevation angle  $\theta_2 \sim U(0, \pi)$  in the  $(x_2, x_3)$  plane. Additionally,  $\theta_3 \sim U(0, \pi/2)$  in the  $(x_3, x_4)$  plane, ensuring that the points remain restricted to a hemisphere. The coordinates are transformed into 4-D Cartesian space:

$$X_1 = \sin(\theta_1) \cos(\theta_2), \quad X_2 = \sin(\theta_1) \sin(\theta_2), \quad X_3 = \cos(\theta_1) \cos(\theta_3), \quad X_4 = \cos(\theta_1) \sin(\theta_3).$$

This produces points on one side of a 4-D unit sphere, effectively generating a 4-D hemisphere. For  $p > 4$ , additional noise dimensions are added to embed the structure in higher dimensions.

```
hemisphere <- gen_hemisphere(n = 1000, p = 4)
```

**Swiss Roll** To further generalize the Swiss roll structure and introduce realistic noise, we define a function `gen_swissroll(n, p, w)`, where  $n$  is the number of points,  $p$  is the total number of dimensions, and  $w$  is the vertical range in the third dimension (Figure 11). The first three dimensions form the classic 3-D Swiss roll shape. The

$$X_1 = t \cos(t), \quad X_2 = t \sin(t), \quad X_3 \sim U(w_1, w_2), \text{ where } t \sim U(0, 3\pi).$$

For  $p > 3$ , the remaining  $p - 3$  dimensions are filled with noise to simulate high-dimensional complexity.

```
swissroll <- gen_swissroll(n = 1000, p = 4, w = c(-1, 1))
```

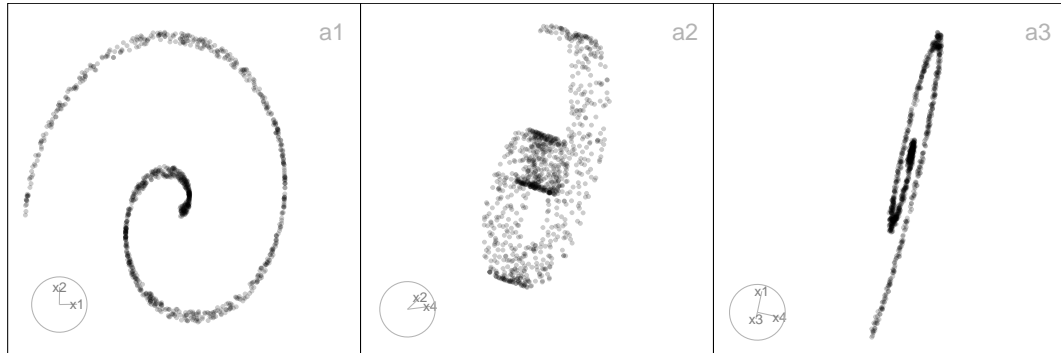


**Figure 11:** Three 2-D projections from 4-D, for the ‘swissroll’ data.

**Trigonometric** Trigonometric-based structures provide flexible ways to simulate complex curved patterns and spirals that often arise in real-world high-dimensional data, such as in biological trajectories, or physical systems (Figure 12). The first few coordinates define the main geometric structure (e.g., crescent, cylinder, spiral, or helix), while for higher-dimensional embeddings, additional noise dimensions are appended: for the crescent shape this occurs when  $p > 2$  (adding  $X_3$  through  $X_p$ ), and for all other trigonometric shapes when  $p > 4$  (adding  $X_5$  through  $X_p$ ). These structures are particularly valuable for testing how well dimension reduction and clustering algorithms preserve intricate geometric and topological features. Table 9 summarizes these functions.

First, the `gen_crescent(n, p)` function generates a  $p$ -dimensional dataset of  $n$  observations based on a 2-D crescent-shaped manifold with optional structured high-dimensional noise (Figure 12 a). Let  $\theta \in [\pi/6, 2\pi]$  be a sequence of  $n$  evenly spaced angles. The corresponding 2-D coordinates are defined by:

$$X_1 = \cos(\theta), \quad X_2 = \sin(\theta).$$

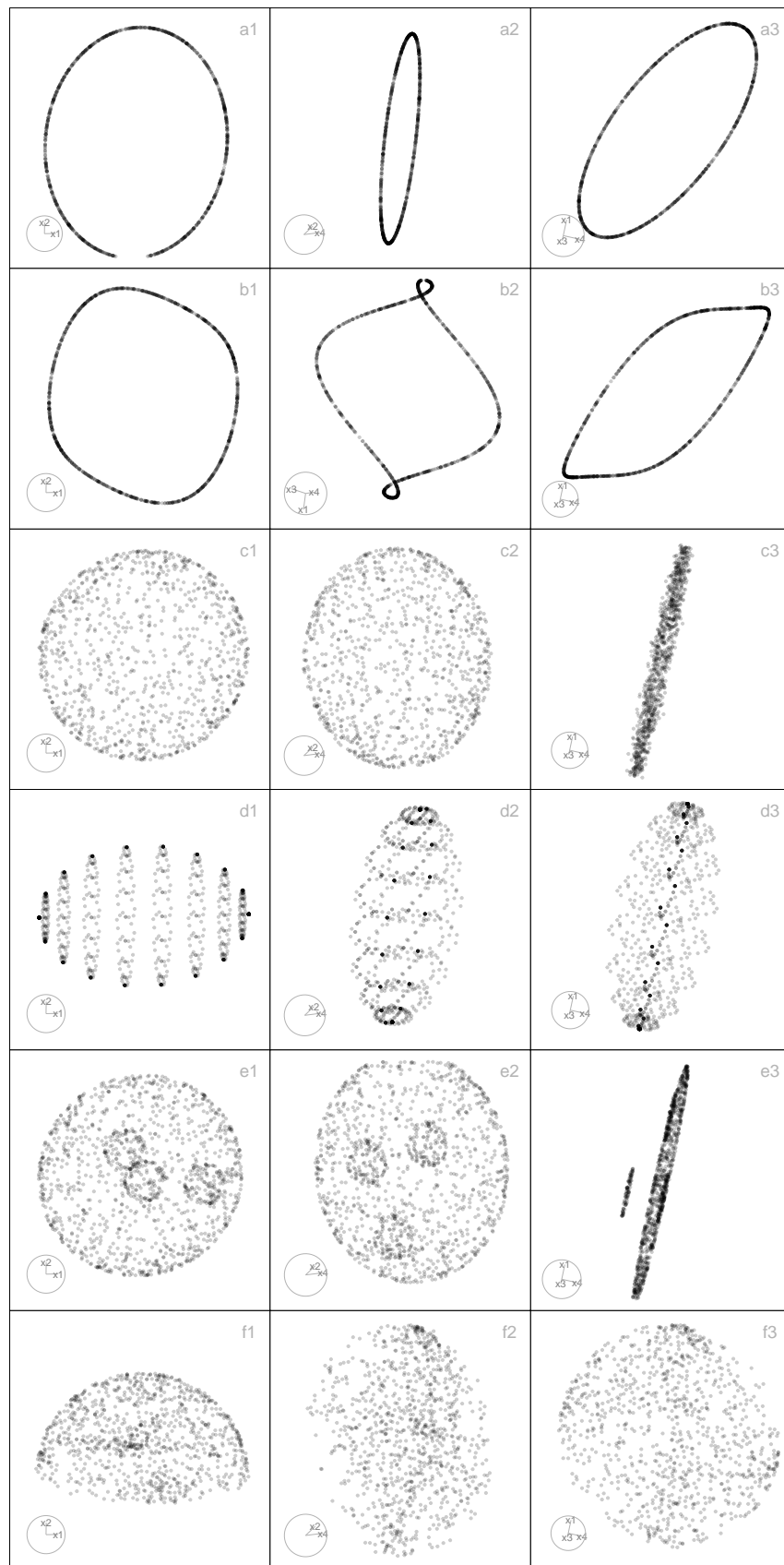


**Figure 10:** Three 2-D projections from 4-D, for the ‘circle’ (a1-a3), ‘curvycycle’ (b1-b3), ‘unifsphere’ (c1-c3), ‘griddedsphere’ (d1-d3), ‘clusteredspheres’ (e1-e3), and ‘hemisphere’ (f1-f3) data.

**Table 9:** cardinalR trigonometric data generation functions

| Function            | Explanation          |
|---------------------|----------------------|
| gen_crescent        | Crescent pattern.    |
| gen_curvycylinder   | Curvy cylinder.      |
| gen_sphericalspiral | Spherical spiral.    |
| gen_helicalspiral   | Helical spiral.      |
| gen_conicspiral     | Conic spiral.        |
| gen_nonlinear       | Nonlinear hyperbola. |

```
crescent <- gen_crescent(n = 1000, p = 4)
```

Second, the `gen_curvycylinder(n, p, h)` function generates a  $p$ -dimensional dataset of  $n$  observations structured as a 3-D cylindrical manifold with an added nonlinear curvy dimension, and optional noise dimensions when  $p > 4$  (Figure 12 b). The core structure consists of a circular base and height values, extended by a nonlinear fourth dimension. Let  $\theta \sim U(0, 3\pi)$  represent a random angle on a circular base and  $z \sim U(0, h)$  represent the height along the cylinder. The coordinates are defined as:  $X_1 = \cos(\theta)$  (Circular base, x-axis),  $X_2 = \sin(\theta)$  (Circular base, y-axis),  $X_3 = z$  (Linear height), and  $X_4 = \sin(z)$  (Nonlinear curvy variation along height).

```
curvycylinder <- gen_curvycylinder(n = 1000, p = 4, h = 10)
```

For a spiraling path on a spherical surface in the first four dimensions, `gen_sphericalspiral(n, p, spins)` (Figure 12 c), let  $\theta \in [0, 2\pi \times \text{spins}]$  be the azimuthal angle (longitude), controls the number of spiral turns and the  $\phi \in [0, \pi]$  be the polar angle (latitude), controls the vertical sweep from the north to the south pole. Cartesian coordinates from spherical conversion:  $X_1 = \sin(\phi) \cos(\theta)$ ,  $X_2 = \sin(\phi) \sin(\theta)$ ,  $X_3 = \cos(\phi) + \epsilon$ , where  $\epsilon \sim U(-0.5, 0.5)$  introduces vertical jitter, and  $X_4 = \theta / \max(\theta)$ : a normalized progression along the spiral path. This generates a spherical spiral curve embedded in 4-D space, combining both circular and vertical movement, with gentle curvature and non-linear progression.

```
sphericalspiral <- gen_sphericalspiral(n = 1000, p = 4, spins = 1)
```

For a helical spiral in four dimensions, `gen_helicalspiral(n, p)` (Figure 12 d), let  $\theta \in [0, 5\pi/4]$  be a sequence of angles controlling rotation around a circle. Cartesian coordinates;  $X_1 = \cos(\theta)$ : circular trajectory along the x-axis,  $X_2 = \sin(\theta)$ : circular trajectory along the y-axis,  $X_3 = 0.05\theta + \epsilon_3$ , with  $\epsilon_3 \sim U(-0.5, 0.5)$ : linear progression (height) with vertical jitter, simulating a helix, and  $X_4 = 0.1 \sin(\theta)$ : oscillates with  $\theta$ , representing a periodic “wobble” along the fourth dimension.

```
helicalspiral <- gen_helicalspiral(n = 1000, p = 4)
```

Similarly, the `gen_conicspiral(n, p, spins)` function generates a dataset of  $n$  points forming a conical spiral in the first four dimensions of  $p$ -D (Figure 12 e). The geometry combines radial expansion, vertical elevation, and spiral deformation, simulating a structure that fans out like a 3-D conic helix. The shape is defined by parameter  $\theta \in [0, 2\pi \text{spins}]$ , controlling the angular progression of the spiral. The Archimedean spiral in the horizontal plane is represented by;  $X_1 = \theta \cos(\theta)$  for radial expansion in x, and  $X_2 = \theta \sin(\theta)$  for radial expansion in y. The growth pattern resembles a cone, with the height increasing according to  $X_3 = 2\theta / \max(\theta) + \epsilon_3$ , with  $\epsilon_3 \sim U(-0.1, 0.6)$ . Spiral modulation in the fourth dimension is represented by  $X_4 = \theta \sin(2\theta) + \epsilon_4$ , with  $\epsilon_4 \sim U(-0.1, 0.6)$  which simulates a twisting helical component in a non-radial dimension.

```
conicspiral <- gen_conicspiral(n = 1000, p = 4, spins = 1)
```

Finally, the `gen_nonlinear(n, p, hc, non_fac)` function simulates a non-linear 2-D surface embedded in higher dimensions, constructed using inverse and trigonometric transformations applied to independent variables (Figure 12 f). The  $X_1 \sim U(0.1, 2)$ : base variable (avoids zero to prevent division errors),  $X_3 \sim U(0.1, 0.8)$ : independent auxiliary variable,  $X_2 = hc/X_1 + \text{nonfac} \sin(X_1)$ : non-linear combination of hyperbolic and sinusoidal transformations, creating sharp curvature and oscillation, and  $X_4 = \cos(\pi X_1) + \epsilon$ , with  $\epsilon \sim U(-0.1, 0.1)$ : additional nonlinear variation based on cosine, simulating more subtle periodic structure. These transformations together result in a non-linear surface warped in multiple ways: sharp vertical shifts due to inverse terms, smooth waves from sine and cosine, and additional jitter.

**Table 10:** cardinalR trefoil data generation functions

| Function      | Explanation                |
|---------------|----------------------------|
| gen_trefoil4d | Trefoil in \$4\text{-}D\$. |
| gen_trefoil3d | Trefoil in \$3\text{-}D\$. |

**Table 11:** cardinalR noise dimensions generation functions

| Function      | Explanation  |
|---------------|--|
| gen_noisedims | Gaussian noise dimensions with optional mean and standard deviation.   |
| gen_wavydims1 | Wavy noise dimensions based on a user-specified theta sequence with added jitter.  |
| gen_wavydims2 | Wavy noise dimensions using polynomial transformations of an existing dimension vector.  |
| gen_wavydims3 | Wavy noise dimensions using a combination of polynomial and sine transformations based on the first three dimensions of a dataset. |

```
nonlinear <- gen_nonlinear(n = 1000, p = 4, hc = 1, non_fac = 0.5)
```

**Trefoil knots** The Trefoil is a closed, nontrivial one-dimensional manifold embedded in 3-D or 4-D space (Figure 13). The trefoil features topological complexity in the form of self-overlaps, making it a valuable test case for evaluating the ability of non-linear dimension reduction methods to preserve global structure, loops, and embeddings in high-dimensional data. Table 10 summarizes these functions.

For the 4-D trefoil knot, the function `gen_trefoil4d(n, p, steps)` generates the structure on the 3-sphere ( $S^3 \subset \mathbb{R}^4$ ) using two angular parameters,  $\theta$  and  $\phi$ . A band of thickness around the knot path is controlled by the `steps` argument, while the number of  $\theta$  and  $\phi$  values is determined by the `steps` and `n` arguments, respectively (Figure 13 a). The coordinates are defined as

$$X_1 = \cos(\theta) \cos(\phi), \quad X_2 = \cos(\theta) \sin(\phi), \quad X_3 = \sin(\theta) \cos(1.5\phi), \text{ and } X_4 = \sin(\theta) \sin(1.5\phi)$$

, where  $\theta$  and  $\phi$  trace the knot's path. For  $p > 4$ , the quadratic structure is embedded into higher dimensions by appending additional noise dimensions.

```
trefoil4d <- gen_trefoil4d(n = 500, p = 4, steps = 5)
```

For the 3-D stereographic projection, `gen_trefoil3d(n, p, steps)` maps each point  $(X_1, X_2, X_3, X_4) \in \mathbb{R}^4$  to

$$(X'_1, X'_2, X'_3) \in \mathbb{R}^3 \text{ using } X'_1 = X_1 / (1 - X_4), \quad X'_2 = X_2 / (1 - X_4), \text{ and } X'_3 = X_3 / (1 - X_4),$$

excluding points where  $X_4 = 1$  to avoid division by zero (Figure 13 b). As with the 4-D case, optional noise dimensions can be added to embed the knot into higher-dimensional spaces.

```
trefoil3d <- gen_trefoil3d(n = 500, p = 4, steps = 5)
```

### Generate noise dimensions

High-dimensional data structures often benefit from the addition of auxiliary noise dimensions, which can be used to assess the robustness of dimensionality reduction and clustering algorithms. The functions in this section provide flexible ways to generate random noise dimensions, ranging from purely random Gaussian variables to more structured, wavy patterns that mimic non-linear distortions in high-dimensional space. These functions can be applied independently or combined with other geometric structures to create complex simulated datasets. Table 11 details these functions.

The `gen_noisedims(n, p, m, s)` function generates  $p$  independent Gaussian noise dimensions,

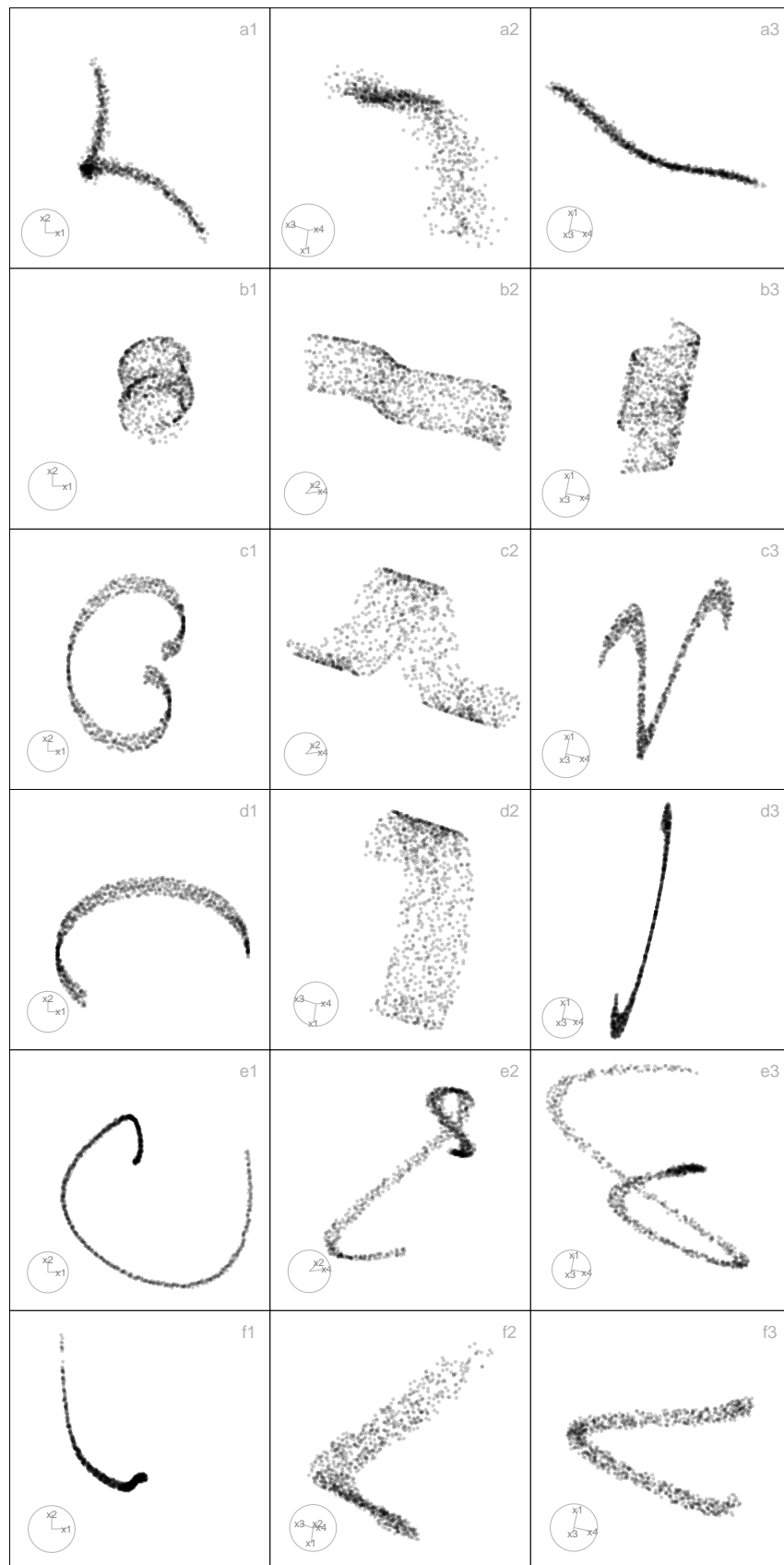


**Figure 12:** Three 2-D projections from 4-D, for the ‘crescent’ (a1-a3), ‘curvycylinder’ (b1-b3), ‘sphericalspiral’ (c1-c3), ‘helicalspiral’ (d1-d3), ‘conicspiral’ (e1-e3), and ‘nonlinear’ (f1-f3) data.

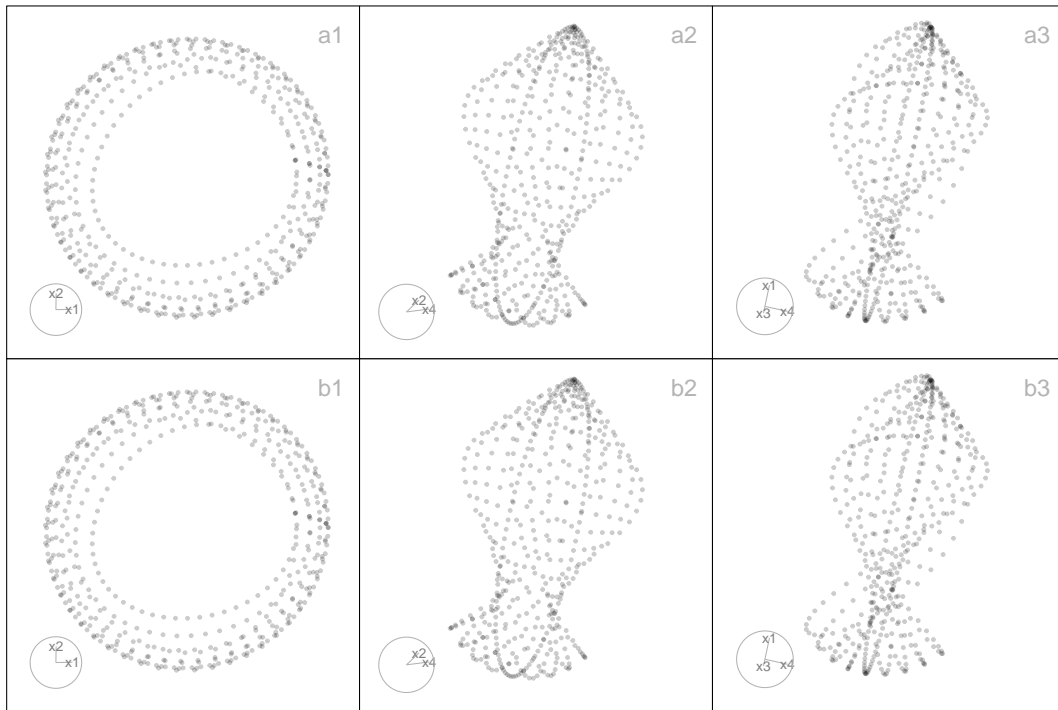


**Figure 13:** Three 2-D projections from 4-D, for the ‘trefoil4d’ (a1-a3) and ‘trefoil3d’ (b1-b3) data.

$$X_j \sim N(m_j, s_j^2), \quad j = 1, \dots, p,$$

with odd-numbered dimensions multiplied by  $-1$  to introduce sign alternation, enhancing variability and decorrelation.

For scenarios where noise should follow a smooth wavy pattern, `gen_wavydims1(n, p, \theta)` generates dimensions as

$$X_j = \alpha_j \theta + \varepsilon_j, \quad \varepsilon_j \sim N(0, \sigma^2), \quad j = 1, \dots, p,$$

where each dimension is scaled by a different factor  $\alpha_j$ , producing structured noise that oscillates along the latent parameter  $\theta$ , mimicking trends or trajectories observed in real-world data.

The `gen_wavydims2(n, p, x_1)` function extends this approach by applying a non-linear transformation to an existing dimension vector  $x_1$ :

$$X_j = \beta_j (-1)^{\lfloor j/2 \rfloor} x_1^{k_j} + \varepsilon_j, \quad j = 1, \dots, p,$$

where  $k_j$  is a randomly chosen polynomial power,  $\beta_j$  is a scaling factor, and  $\varepsilon_j$  is small uniform noise.

Finally, `gen_wavydims3(n, p, \text{data})` generates noise for datasets with multiple correlated dimensions. The first three dimensions are small perturbations of the original coordinates  $(X_1, X_2, X_3)$ , while higher dimensions are constructed via non-linear combinations, including polynomial and trigonometric transformations, e.g.,

$$X_j = f_j(X_1, X_2, X_3) + \varepsilon_j, \quad j > 3,$$

producing high-dimensional noise that preserves some geometric correlation with the base structure while introducing additional complexity.

### Multiple cluster examples

By using the shape generators mentioned above, we can create various examples of multiple clusters. The package includes some of these examples, which are described in Table 12.

**Table 12:** cardinalR multiple clusters generation functions

| Function              | Explanation  |
|-----------------------|--|
| make_mobiusgau        | Möbius-like cluster combined with a Gaussian cluster.          |
| make_multigau         | Multiple Gaussian clusters in high-dimensional space.          |
| make_curvygau         | Curvilinear cluster with a Gaussian cluster.                   |
| make_klink_circles    | K-link circular clusters (non-linear circular patterns).       |
| make_chain_circles    | Chain-like circular clusters connected sequentially.           |
| make_klink_curvycycle | K-link curvy cycle clusters (curvilinear loop structures).     |
| make_chain_curvycycle | Chain-like curvy cycle clusters connected sequentially.        |
| make_gaucircles       | Circular clusters with a Gaussian cluster in the middle.       |
| make_gaucurvycycle    | Curvy circular clusters with a Gaussian cluster in the middle. |
| make_onegrid          | Single grid in two dimensions.                                 |
| make_twogrid_overlap  | Two overlapping grids.   |
| make_twogrid_shift    | Two grids shifted relative to each other.                      |
| make_shape_para       | Parallel shaped clusters.                                      |
| make_three_clust_     | Three clusters with different shapes. (eg:- 01, 02, ..., 20)   |

**Table 13:** cardinalR additional functions

| Function          | Explanation   |
|-------------------|---|
| gen_bkgnoise      | Adds background noise.  |
| randomize_rows    | Randomizes the rows.  |
| relocate_clusters | Relocates the clusters.   |
| gen_nproduct      | Generates a vector of positive integers whose product is approximately equal to a target value.   |
| gen_nsum          | Generates a vector of positive integers whose summation is approximately equal to a target value. |
| gen_rotation      | Generates rotations.  |
| normalize_data    | Normalizes data.  |

## Additional functions

The package includes various supplementary tools in addition to the shape generating functions mentioned earlier. These tools allow users to create background noise, randomize the rows of the data, relocate clusters, generate a vector whose product and sum are approximately equal to a target value, rotate structures, and normalize the data. Table 13 details these functions.

## 3 Application

This section illustrates the use of package by generating a synthetic dataset to evaluate the performance of six popular dimension reduction techniques: Principal Component Analysis (PCA) (Jolliffe, 2011), t-distributed stochastic neighbor embedding (tSNE) (Maaten and Hinton, 2008), uniform manifold approximation and projection (UMAP) (McInnes et al., 2018), potential of heat-diffusion for affinity-based trajectory embedding (PHATE) algorithm (Moon et al., 2019), large-scale dimensionality reduction Using triplets (TriMAP) (Amid and Warmuth, 2019), and pairwise controlled manifold approximation (PaCMAP) (Wang et al., 2021).

The following code generates a dataset of five clusters, positioned with equal inter-cluster distances

in 4-D space (Figure 14).

```
positions <- geozoo::simplex(p=4)$points
positions <- positions * 0.8

## To generate data
five_clusts <- gen_multiclus(n = c(2250, 1500, 750, 1250, 1750), p = 4, k = 5,
                               loc = positions,
                               scale = c(0.4, 0.35, 0.3, 1, 0.3),
                               shape = c("helicalspiral", "hemisphere", "unifcube",
                                         "cone", "gaussian"),
                               rotation = NULL,
                               is_bkg = FALSE)
```

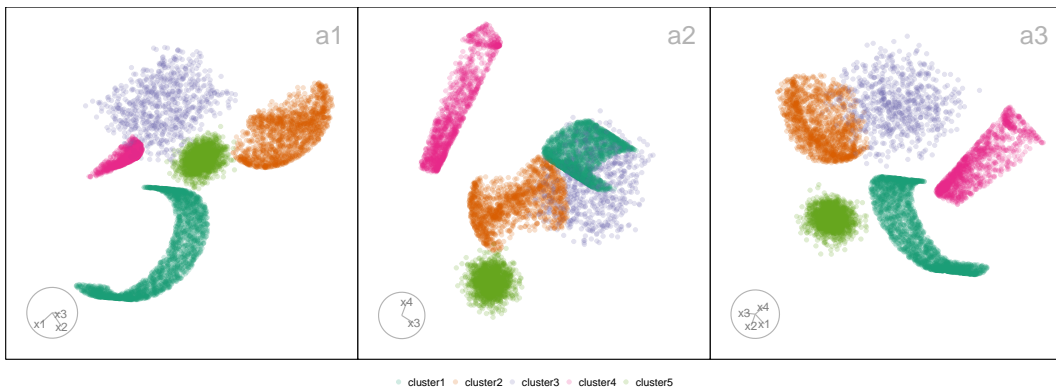


**Figure 14:** Three 2-D projections from 4-D, for the five clusters data. The helical spiral cluster is represented in dark green, the hemisphere cluster in orange, the uniform cube-shaped cluster in purple, the blunted cone cluster in pink, and the Gaussian-shaped cluster in light green.

The five clusters have different geometric structures and each contain different number of points. Specifically, the helical spiral cluster includes 2250 points and was generated with a scale parameter of 0.4. The hemisphere cluster consists of 1500 points with a scale parameter of 0.35. The uniform cube-shaped cluster contains 750 points and uses a scale parameter of 0.3. The blunted cone cluster includes 1250 points, generated with a scale parameter of 1. Finally, the Gaussian-shaped cluster contains 1750 points and was generated with a scale parameter of 0.3.

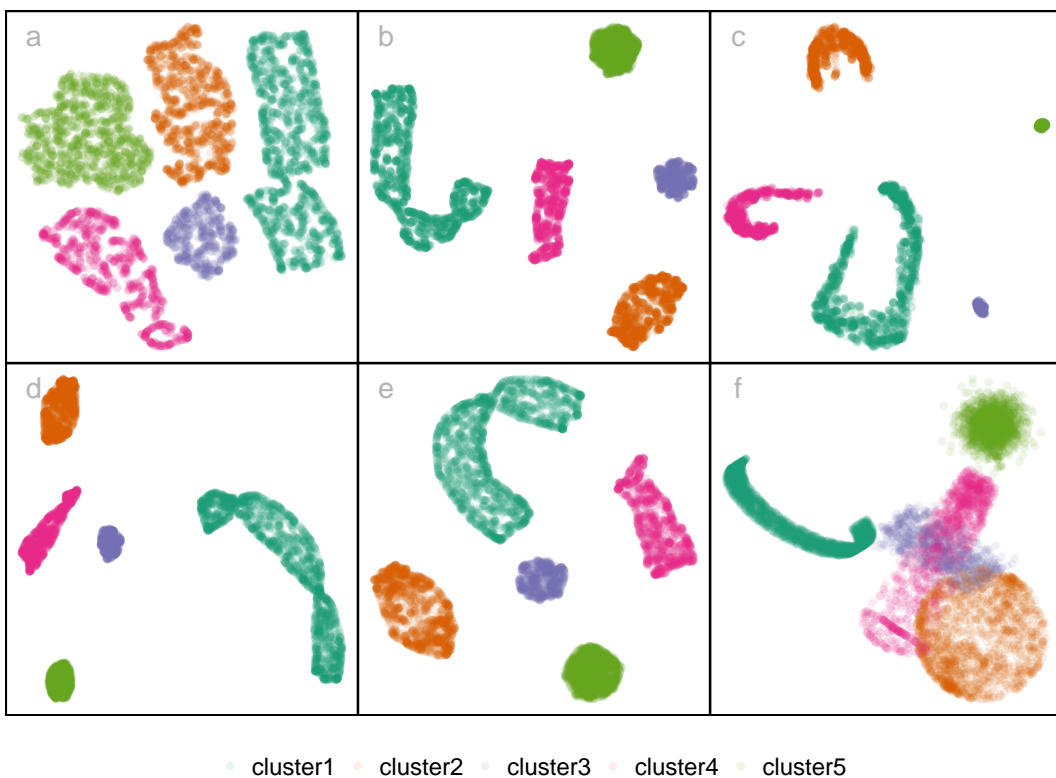


**Figure 15:** Six different dimension reduction representations of the five clusters data using default hyperparameter settings: (a) tSNE, (b) UMAP, (c) PAHTE, (d) TriMAP, (e) PaCMAP, and (f) PCA.

UMAP, PHATE, TriMAP, and PaCMAP effectively separate the five clusters and show the preservation of the global structure (Figure 15). However, PHATE reveals three non-linear clusters, even though two of them do not show non-linearity. UMAP, TriMAP, and PaCMAP successfully maintain the local structures of the data. In contrast, tSNE divides the non-linear cluster into sub-clusters. Also, tSNE fails to preserve the distances between the clusters. PCA, on the other hand, preserves the local structures of the clusters, but some clusters are incorrectly merged that should remain distinct.

## 4 Conclusion

The cardinalR package introduces a flexible framework for generating high-dimensional data structures with well-defined geometric properties. It addresses an important need in the evaluation of clustering, machine learning, and dimensionality reduction (DR) methods by enabling the construction of customized datasets with interpretable structures, noise characteristics, and clustering arrangements. In this way, cardinalR complements existing packages such as geozoo, snedata, and mlbench, while extending the scope to higher dimensions and more complex shapes.

The included structures cover a wide range of diagnostic settings. Branching shapes facilitate the study of continuity and topological preservation, the Scurve with a hole allows investigation of incomplete manifolds, and clustered spheres assess separability on curved surfaces. The Möbius strip introduces challenges from non-orientable geometry, while gridded cubes and pyrholes test spatial regularity and clustering in sparse, non-convex regions.

These structures are designed to support not only algorithm diagnostics, but also teaching high-dimensional concepts, benchmarking reproducibility, and evaluating hyperparameter sensitivity. By allowing users to adjust dimensionality, sample size, noise, and clustering properties, the package promotes transparent experimentation and comparative model evaluation.

Future extensions of cardinalR may include biologically inspired or application-driven data structures would further broaden its utility in domains such as bioinformatics, forensic science, and spatial analysis.

## 5 Acknowledgements

The source material for this paper is available at <https://github.com/JayaniLakshika/paper-cardinalR>.

These R packages were used for this work: `cli` (Csárdi, 2025), `tibble` (Müller and Wickham, 2023), `gtools` (Warnes et al., 2023), `dplyr` (Wickham et al., 2023), `stats` (R Core Team, 2025), `tidyverse` (Wickham et al., 2024), `purrr` (Wickham and Henry, 2025), `mvtnorm` (Genz and Bretz, 2009), `geozoo` (Schlöerke, 2016), and `MASS` (Venables and Ripley, 2002). This article is created using `knitr` (Xie, 2015) and `rmarkdown` (Xie et al., 2018) in R with the `rjtools::rjournal_article` template.

## Bibliography

- E. Amid and M. K. Warmuth. Trimap: Large-scale dimensionality reduction using triplets. *ArXiv*, abs/1910.00204, 2019. URL <https://api.semanticscholar.org/CorpusID:203610264>. [p20]
- G. Csárdi. *cli: Helpers for Developing Command Line Interfaces*, 2025. URL <https://CRAN.R-project.org/package=cli>. R package version 3.6.4. [p23]
- A. Genz and F. Bretz. *Computation of Multivariate Normal and t Probabilities*. Lecture Notes in Statistics. Springer-Verlag, Heidelberg, 2009. ISBN 978-3-642-01688-2. [p23]
- I. Jolliffe. *Principal Component Analysis*, pages 1094–1096. Springer Berlin Heidelberg, Berlin, Heidelberg, 2011. ISBN 978-3-642-04898-2. doi: 10.1007/978-3-642-04898-2\_455. URL [https://doi.org/10.1007/978-3-642-04898-2\\_455](https://doi.org/10.1007/978-3-642-04898-2_455). [p20]
- F. Leisch and E. Dimitriadou. *mlbench: Machine Learning Benchmark Problems*, 2024. URL <https://CRAN.R-project.org/package=mlbench>. R package version 2.1-6. [p1]
- L. V. D. Maaten and G. E. Hinton. Visualizing data using t-sne. *Journal of Machine Learning Research*, 9: 2579–2605, 2008. [p20]
- L. McInnes, J. Healy, N. Saul, and L. Großberger. Umap: Uniform manifold approximation and projection. *Journal of Open Source Software*, 3(29):861, 2018. doi: 10.21105/joss.00861. URL <https://doi.org/10.21105/joss.00861>. [p20]
- J. Melville. *sne: SNE Simulation Dataset Functions*, 2025. URL <https://github.com/jlmelville/sne>. R package version 0.0.0.9001, commit beebcf91c365bf5006be08fb614585b4659c05c5. [p1]
- K. R. Moon, D. van Dijk, Z. Wang, S. A. Gigante, D. B. Burkhardt, W. S. Chen, K. Yim, A. van den Elzen, M. J. Hirn, R. R. Coifman, N. B. Ivanova, G. Wolf, and S. Krishnaswamy. Visualizing structure and transitions in high-dimensional biological data. *Nature Biotechnology*, 37:1482–1492, 2019. [p20]
- K. Müller and H. Wickham. *tibble: Simple Data Frames*, 2023. URL <https://CRAN.R-project.org/package=tibble>. R package version 3.2.1. [p23]
- R Core Team. *R: A Language and Environment for Statistical Computing*. R Foundation for Statistical Computing, Vienna, Austria, 2025. URL <https://www.R-project.org/>. [p23]
- B. Schloerke. *geozoo: Zoo of Geometric Objects*, 2016. URL <https://CRAN.R-project.org/package=geozoo>. R package version 0.5.1. [p1, 23]
- C. Trapnell, D. Cacchiarelli, J. Grimsby, P. Pokharel, S. Li, M. Morse, N. J. Lennon, K. J. Livak, T. S. Mikkelsen, and J. L. Rinn. The dynamics and regulators of cell fate decisions are revealed by pseudotemporal ordering of single cells. *Nature Biotechnology*, 32(4):381–386, 2014. doi: 10.1038/nbt.2859. URL <https://doi.org/10.1038/nbt.2859>. [p2]
- W. N. Venables and B. D. Ripley. *Modern Applied Statistics with S*. Springer, New York, fourth edition, 2002. URL <https://www.stats.ox.ac.uk/pub/MASS4/>. ISBN 0-387-95457-0. [p23]
- Y. Wang, H. Huang, C. Rudin, and Y. Shaposhnik. Understanding how dimension reduction tools work: An empirical approach to deciphering t-sne, umap, trimap, and pacmap for data visualization. *Journal of Machine Learning Research*, 22(201):1–73, 2021. URL <http://jmlr.org/papers/v22/201061.html>. [p20]
- G. R. Warnes, B. Bolker, T. Lumley, A. Magnusson, B. Venables, G. Rydon, and S. Moeller. *gtools: Various R Programming Tools*, 2023. URL <https://CRAN.R-project.org/package=gtools>. R package version 3.9.5. [p23]

- H. Wickham and L. Henry. *purrr: Functional Programming Tools*, 2025. URL <https://CRAN.R-project.org/package=purrr>. R package version 1.0.4. [p23]
- H. Wickham, R. François, L. Henry, K. Müller, and D. Vaughan. *dplyr: A Grammar of Data Manipulation*, 2023. URL <https://CRAN.R-project.org/package=dplyr>. R package version 1.1.4. [p23]
- H. Wickham, D. Vaughan, and M. Girlich. *tidyR: Tidy Messy Data*, 2024. URL <https://CRAN.R-project.org/package=tidyr>. R package version 1.3.1. [p23]
- Y. Xie. *Dynamic Documents with R and knitr*. Chapman and Hall/CRC, Boca Raton, Florida, 2nd edition, 2015. URL <https://yihui.name/knitr/>. ISBN 978-1498716963. [p23]
- Y. Xie, J. Allaire, and G. Grolemund. *R Markdown: The Definitive Guide*. Chapman and Hall/CRC, Boca Raton, Florida, 2018. URL <https://bookdown.org/yihui/rmarkdown>. ISBN 978-1138359338. [p23]
- L. Zappia, B. Phipson, and A. Oshlack. Splatter: simulation of single-cell rna sequencing data. *Genome Biology*, 2017. doi: 10.1186/s13059-017-1305-0. URL <http://dx.doi.org/10.1186/s13059-017-1305-0>. [p1]

*Jayani P. Gamage*  
Monash University  
Department of Econometrics and Business Statistics, VIC 3800 Australia  
<https://jayanilakshika.netlify.app/>  
ORCID: 0000-0002-6265-6481  
[jayani.piayadigamage@monash.edu](mailto:jayani.piayadigamage@monash.edu)

*Dianne Cook*  
Monash University  
Department of Econometrics and Business Statistics, VIC 3800 Australia  
<http://www.dicook.org/>  
ORCID: 0000-0002-3813-7155  
[dicook@monash.edu](mailto:dicook@monash.edu)

*Paul Harrison*  
Monash University  
MGBP, BDInstitute, VIC 3800 Australia  
ORCID: 0000-0002-3980-268X  
[paul.harrison@monash.edu](mailto:paul.harrison@monash.edu)

*Michael Lydeamore*  
Monash University  
Department of Econometrics and Business Statistics, VIC 3800 Australia  
ORCID: 0000-0001-6515-827X  
[michael.lydeamore@monash.edu](mailto:michael.lydeamore@monash.edu)

*Thiyanga S. Talagala*  
University of Sri Jayewardenepura  
Department of Statistics, Gangodawila, Nugegoda 10100 Sri Lanka  
<https://thiyanga.netlify.app/>  
ORCID: 0000-0002-0656-9789  
[ttalagala@sjp.ac.lk](mailto:ttalagala@sjp.ac.lk)